J. Synchrotron Rad. (1998). **5**, 860–862

# A multiwire proportional counter for very high counting rates

**A. F. Barbosa,[a*] G. P. Guedes,[a] E. Tamura,[b] I. M. Pepe[c] and N. B. Oliveira[c]**

*[a]CBPF, Rua Dr Xavier Sigaud 150, CEP 22290-180, Rio de Janeiro, RJ, Brazil, [b]LNLS, CP 6192, CEP 13083-970, Campinas, SP, Brazil, and [c]UFBA, Campus de Ondina, CEP 40210-340, Salvador, BA, Brazil. E-mail: laudo@cat.cbpf.br*

(*Received 4 August 1997; accepted 1 December 1997*)

Preliminary measurements in a proportional counter with two independently counting wires showed that counting rates up to $10^6$ counts $s^{-1}$ $wire^{-1}$ can be reached without critical loss in the 'true *versus* measured' linearity relation. Results obtained with a detector containing 30 active wires (2 mm pitch) are presented. With each wire is associated a fast pre-amplifier and a discriminator channel. Global counting rates in excess of $10^7$ events $s^{-1}$ are reported. Dead-time losses are corrected by use of simple mathematical-modelling functions. Data-acquisition systems are described for one-dimensional (real-time) and two-dimensional (off-line) position-sensitive detection systems.

**Keywords: multiwire proportional counters; X-ray detectors; high counting rates; dead time.**

## 1. Introduction

The availability of high-intensity X-ray sources, especially synchrotron radiation sources, has established the need for the development of high-counting-rate detectors. Although integrating detectors can cope with high counting rates, some of their features (*e.g.* intrinsic noise, low sensitivity to small intensity variations and to the energy of detected particles) often limit their applicability. Recent developments on avalanche photodiode detectors have resulted in photon-counting devices with a dynamic range extending from $10^{-2}$ to $10^7$ counts $s^{-1}$ (Kishimoto, 1995; Toellner *et al.*, 1994). This is due to the combination of a solid-state detecting medium with a relatively high avalanche gain (Farrell *et al.*, 1994). However, these are low-size detectors, with usually less than 1 $cm^2$ active surface, and may not easily replace large area detectors. Silicon (Pullia *et al.*, 1995) and plastic scintillator (Radtke, 1990) detectors have also been reported for counting rates above $10^6$ counts $s^{-1}$.

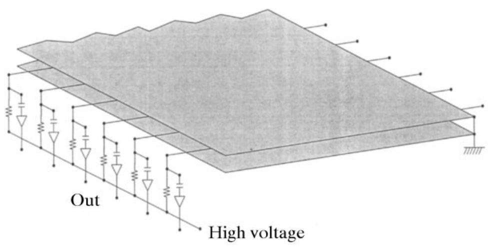


**Figure 1**
Schematic view of the detector, illustrating the connection of the wires to the pre-amplifiers and to the high voltage supply.

In the field of gas detectors, it is known that the space charge resulting from exposure to high fluxes ultimately limits their counting-rate capability by reducing the electric field in the active region. Some issues have been addressed to bypass this limitation, essentially based on the reduction of the drift path for electrons and ions: microstrip (Oed, 1988), microgap (Hall *et al.*, 1995) and microdot (Biagi *et al.*, 1995) detectors. Very high counting rates may be obtained in a multiwire proportional counter (MWPC) by appropriate choice of geometric parameters, gas filling, and signal processing electronics (Fischer *et al.*, 1985, 1986). The work presented here illustrates that an MWPC could handle relatively high counting rates even in moderate operating conditions.

## 2. Detector

In a prototype detector with two wires, we have observed that each wire can reach counting rates up to $10^6$ counts $s^{-1}$ without critical dead-time losses. The counting-rate capability of an MWPC could therefore be extended well above $10^6$ counts $s^{-1}$ as long as the wires operate independently. The saturation counting rate depends on the detector geometry: mainly the wire pitch and the anode-to-cathode gap. If the wires operate as parallel counters, a compromise could be found that sets the counting limit to an acceptable level for a given application. In order to evaluate this possibility, we have built a detector with 33 wires, four of which are guard wires and 29 are active counters. The wire plane lies in between two cathode planes. The wire pitch is 2 mm, and the gap from anode wire plane to cathode planes is 3.2 mm. The detecting area is $6 \times 6$ cm and the diameter of the active wires is 20 μm.

Anode wires are set to a high voltage relative to cathode planes, and avalanche signals are capacitively decoupled and connected to a voltage pre-amplifier (Fig. 1). The 'RC' product defining the pre-amplifier's time-shaping constant is lower than the inverse of the expected counting rate ($RC \simeq 200$ ns). A leading-edge discriminator provides a logic signal for each detected photon.

One of the cathode planes is a 300 μm carbon-fibre window through which X-ray photons enter the detecting region. For the results shown in the following section, the operating gas was Ar + 10% $CH_4$, 0.2 atm above normal pressure.

## 3. Results

The detector stability, linearity and spatial resolution have been characterized with the direct beam of a Cu-target X-ray generator, filtered and attenuated with Ni sheets. An $^{55}$Fe source has also been used for stability measurements. In order to check the spatial resolution, the beam profile of the XAFS beamline at LNLS has been scanned.

### 3.1. *Stability*

By illuminating the detector with an $^{55}$Fe source and varying the distance from the source to the detector, it has been checked that the detection system was stable for counting rates up to $10^5$ counts $s^{-1}$ $wire^{-1}$. For higher rates, *i.e.* $10^6$ counts $s^{-1}$ $wire^{-1}$, the X-ray generator was used and the output counting rate of a wire was verified to remain stable, within 0.15% of the average, for more than the time taken to carry out other characterization measurements (>1 h).

### 3.2. *Linearity*

The linearity relation between the true and the measured counting rates has been evaluated by conveniently attenuating the X-ray beam, so that a range $10^3$–$10^6$ counts $s^{-1}$ wire$^{-1}$ has been covered. Subdivisions of this range have been accessed by regularly varying the X-ray tube current.

Counting-rate measurements from one central wire are plotted in Fig. 2. It is clear from the figure that dead-time losses are important above $\sim 10^5$ counts $s^{-1}$. However, since the wires are independent parallel counters, the detection system as a whole is able to process a much higher counting rate. By assuming that the true rate of photons incident to the wire is linearly proportional to the X-ray tube current (and zero at zero current), we have estimated the true counting rate from the measured data by supposing a non-paralyzable behaviour for the dead-time losses (see §4). This estimation has only been possible for the first three sets of data in Fig. 2, since no simple mathematical model was applicable for measured counting rates above $10^6$ counts $s^{-1}$. Fig. 3 illustrates the true *versus* measured counting-rate behaviour up to this rate. The best linearity between X-ray tube current and estimated true counting rate has been obtained with a dead-time value of 715 ns.

In Fig. 4 the beam intensity profile is shown as a function of the X-ray tube current. As the beam intensity increases, deviations from the linear behaviour are clearly seen, since individual wires do not stand counting rates in excess of $10^6$ counts $s^{-1}$. On the other hand, overall counting rates above $2 \times 10^7$ counts $s^{-1}$ were measured at 37.5 mA X-ray tube current. Corrections to the recorded data are discussed in §4.

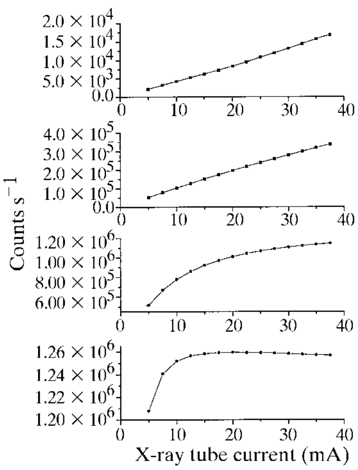


**Figure 2**
Plots of the linearity measurements for one wire, with counting rates extending from $10^3$ to $10^6$ counts $s^{-1}$.

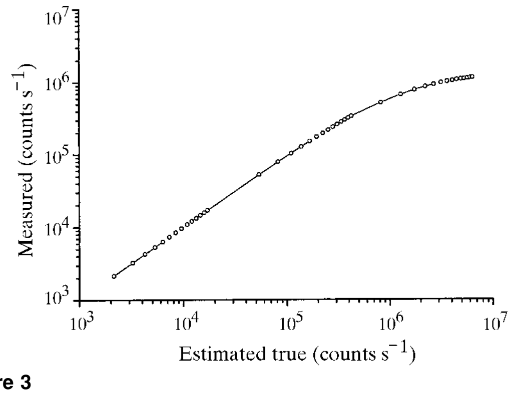


**Figure 3**
True *versus* measured counting-rate relation for one wire, estimated from the first three sets of data in Fig. 2 by use of a non-paralyzable dead-time model function.

### 3.3. *Spatial resolution*

With the wires operating independently, the detector may be considered as position-sensitive to one dimension. The spatial resolution is in this case determined by the wire pitch (2 mm). Fig. 5 shows the beam intensity profile of the LNLS XAFS beamline in the vertical direction. The beam width in this direction was known to be 1 mm. The beam was monochromated to 6.5 keV and attenuated by Ti sheets. As expected, the profile in Fig. 5 indicates a maximum counting rate in one of the wires, while the other wires detect scattered radiation.

## 4. Correction for dead-time losses

We have attempted to correct the data shown in Fig. 4 for dead-time losses. A calibration of the true counting rate incident to each wire was needed, and for this purpose we have assumed that the detection system response is linear for low counting rates ($10^3$–$10^4$ counts $s^{-1}$ wire$^{-1}$). This is a reasonable assumption, as confirmed by the data in Fig. 2. By taking a set of data for one of the wires in which the counting rate ranges from $10^4$ to $10^5$ counts $s^{-1}$, it has been possible to estimate the dead time of the detection system. Three mathematical models have been used (Knoll, 1989): $y_{np} = x/(1 + x\tau)$, $y_{lr} = x(1 - x\tau)$, $y_p = x\exp(-x\tau)$, where subscripts *np*, *lr* and *p* indicate the non-paralyzable, low-rate and paralyzable models, respectively; $y$ and $x$ are the

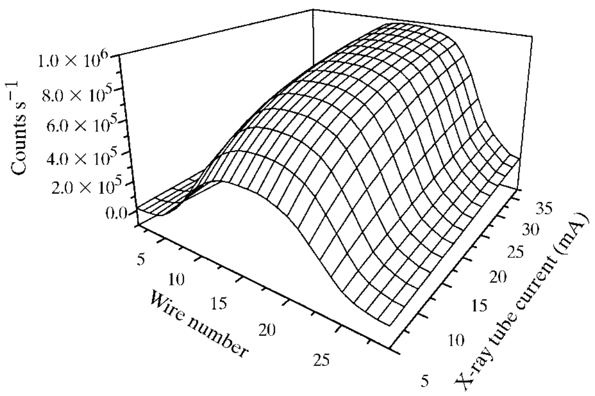


**Figure 4**
Beam intensity profile as a function of the X-ray tube current.

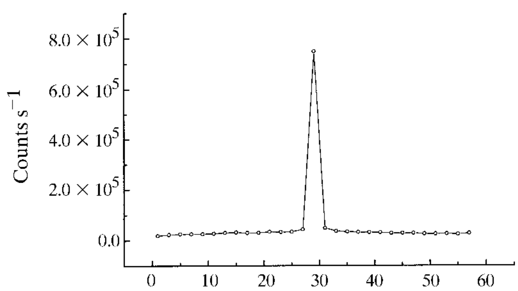


**Figure 5**
Attenuated synchrotron radiation beam intensity profile, obtained at the XAFS beamline of the LNLS.

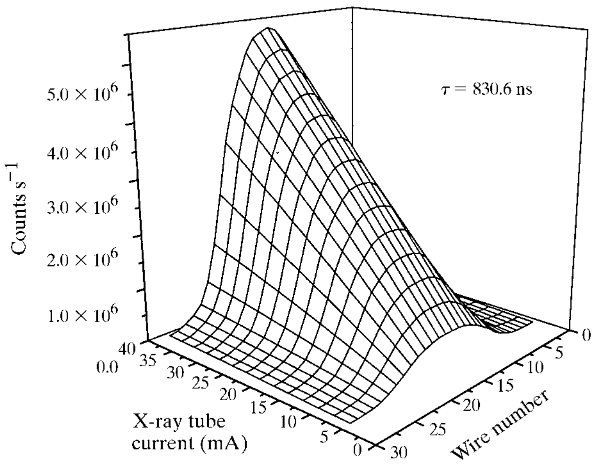


**Figure 6**
Correction to data in Fig. 4, obtained from a non-paralyzable mathematical model with $\tau = 830.6$ ns.

measured and the true counting rates, respectively, and $\tau$ is the dead time. The low-rate model function is the one to which both the paralyzable and non-paralyzable functions tend to when the counting rate is very low ($\ll 1/\tau$). Fitting these functions to the set of data we have found $\tau_{np} = 835.5$ ns, $\tau_{lr} = 758.8$ ns and $\tau_p = 796.5$ ns. These values are higher than the one obtained in §3.2, and may be attributed to the fact that in the present case the X-ray beam is distributed over the whole detector instead of a single wire.

The last two plots in Fig. 2 suggest that, at $\sim 10^6$ counts s$^{-1}$ wire$^{-1}$, the detection-system behaviour is closer to a non-paralyzable model, since the measured counting rate does not decrease as it would in a paralyzable model. By inverting $y_{np}$ it has been possible to correct the whole data set. Fig. 6 shows corrected data obtained for $\tau = 830.6$ ns.

## 5. Data-acquisition system

A complete data-acquisition system for the detector includes a pre-amplifier, a discriminator and a counter for each of the active wires. A control unit must also be provided for assembling information of the whole detector and storing data in memory. Such a system is presently under development at LNLS. The analog part will be composed of pre-amplifiers and discriminators, already developed. These shall be upgraded to provide faster signals (<100 ns duration) and consequently higher counting rates. The counters and the control unit will be implemented using standard NIM technology. Use of field programmable gate array (FPGA) logic allows packing of up to 30 counters per module. The control unit communicates with each module, *via* a private bus, and with an IBM-PC-compatible microcomputer that displays data in real time. A complete description of the system will be presented in the near future.

Two-dimensional position-sensitive detectors and the associated data-acquisition systems have been prepared for use in a high-energy physics experiment at Fermilab, USA (Anjos *et al.*, 1997). In this case, two orthogonal cathode wire planes are included in the detector for sampling the avalanche signals in the $X$ and $Y$ directions. Signals from anode and cathode wires are treated and sent to a controlling unit that latches the state of all the wires whenever a master gate signal triggers an event (namely charm photoprodution). The latched data is registered in memory and processed off-line by an image-reconstruction algorithm.

## 6. Conclusions

The detector presented here is an MWPC in which the wires have been used as independent photon counters. Although the saturation counting rate for each wire is limited to about $10^6$ counts s$^{-1}$, the detector as a whole has been able to process $\sim 3 \times 10^7$ counts s$^{-1}$. The limit in counts s$^{-1}$ wire$^{-1}$ is due to the space charge effect (Smith & Mathieson, 1987), and also to the fact that the used readout electronics are relatively slow, implying dead-time losses. As mentioned in §5, the pre-amplifier and the discriminator circuits shall be upgraded in the data-acquisition system under development. In order to cope with higher counting rates, the detector geometry might be improved (lower anode-to-cathode gap), and a more appropriate filling gas could be used. Counting rates close to $10^7$ counts s$^{-1}$ wire$^{-1}$ have been reported (Fischer *et al.*, 1985).

The construction of the detector and data-acquisition system has been possible thanks to financial support by PADCT/CNPq and FAPESP (Brazilian research funding agencies).

## References

Anjos, J. C., Barbosa, A. F., Oliveira, N. B., Pepe, I. M. & Simão, F. R. A. (1997). *Proceedings of the First Latin American Symposium on High Energy Physics*, edited by J. C. D'Olivo & M. Klein. American Institute of Physics.
Biagi, S. F., Bordas, J., Duxbury, D., Gabathuler, E., Jones, T. J. & Kiourkos, S. (1995). *Nucl. Instrum. Methods*, A**366**, 76–78.
Farrell, R., Vanderpuye, K., Cirignano, L., Squillante, M. R. & Entine, G. (1994). *Nucl. Instrum. Methods*, A**353**, 176–179.
Fischer, J., Hrisoho, A., Radeka, V. & Rehak, P. (1985). *Nucl. Instrum. Methods*, A**238**, 249–264.
Fischer, J., Radeka, V. & Smith, G. C. (1986). *Nucl. Instrum. Methods*, A**246**, 511–516.
Hall, C. J., Lewis, A., Parker, B., Sheldon, J., Fore, N. S., Helsby, W. & Jones, A. (1995). *Nucl. Phys. B (Proc. Suppl.)*, **44**, 242–245.
Kishimoto, S. (1995). *Rev. Sci. Instrum.* **66**(2), 2314–2316.
Knoll, G. F. (1989). *Radiation Detection and Measurement.* 2nd ed. New York: John Wiley.
Oed, A. (1988). *Nucl. Instrum. Methods*, A**263**, 351.
Pullia, A., Kraner, H. W., Siddons, D. P., Furenlid, L. R. & Bertuccio, G. (1995). *IEEE Trans. Nucl. Sci.* **42**(4), 585–589.
Radtke, J. (1990). Technical note 322. Siemens Analytical X-ray Instruments Inc., Madison, Wisconsin, USA.
Smith, G. C. & Mathieson, E. (1987). *IEEE Trans. Nucl. Sci.* **34**, 410–413.
Toellner, T. S., Sturhahn, W., Alp, E. E., Montane, P. A. & Ramanathan, M. (1994). *Nucl. Instrum. Methods*, A**350**, 595–600.